Microcavity Polariton Splitting of Intersubband Transitions

Dimitri Dini,[1] Rüdeger Köhler,[1] Alessandro Tredicucci,[1,*] Giorgio Biasiol,[2] and Lucia Sorba[2,3]

[1]*NEST-INFM and Scuola Normale Superiore, Piazza dei Cavalieri 7, I-56126 Pisa, Italy*

[2]*NEST-INFM and Laboratorio Nazionale TASC-INFM, AREA Science Park, SS 14 Km 163.5, Basovizza, I-34012 Trieste, Italy*

[3]*Università di Modena e Reggio Emilia, Via Campi 213/A, I-41100 Modena, Italy*

(Received 11 November 2002; published 18 March 2003)

The optical response of the intersubband excitation of multiple two-dimensional electron gases within a semiconductor microcavity has been studied through angle-dependent reflectance measurements. Using a resonator based on total internal reflection, a clear splitting of about 14 meV of the coupled intersubband cavity modes is observed from 10 K to room temperature, with resulting polaritonlike dispersion. The experimental findings are in good agreement with theoretical calculations performed in a transfer-matrix formalism.

DOI: 10.1103/PhysRevLett.90.116401 PACS numbers: 71.36.+c, 42.50.–p, 73.21.Fg, 78.67.De

The interaction of light with material excitations can be completely altered in microcavity structures where the electromagnetic field is confined and the photonic density of states deeply modified. In particular, if the coupling between the optical transition and the radiation is sufficiently strong compared to the damping rates, new elementary excitations, eigenstates of the full photon-matter Hamiltonian, take form, usually named ''cavity polaritons.'' They present a characteristic anticrossing behavior, with a mode separation often referred to as ''vacuum-field Rabi splitting,'' in analogy to the well-known Rabi splitting of saturable two-level systems. The study of these phenomena started some time ago in atomic physics [1] and is still attracting a lot of interest especially in connection to research on quantum computation [2]. In the semiconductor world, cavity electrodynamics has developed mainly in conjunction with excitonic states, albeit in a variety of systems, from quantum wells (QWs) [3–6] to bulk [7], from III-V compounds to II-VI [8]. It is currently a very active field, thanks mostly to the latest advances concerning polariton parametric amplification [9] and exciton condensation [10].

Intersubband transitions between confined electronic levels within the conduction band of a semiconductor heterostructure are becoming more and more relevant in understanding the physics of collective excitations of the two-dimensional electron gas (2DEG) [11] and are finding successful application in a number of photonic devices, such as QW infrared photodetectors [12] and quantum cascade lasers [13,14]. Their interaction with cavity photons in microresonators has however remained a largely unexplored subject, if not for a few works on whispering gallery disk lasers [15]. There are in fact various practical difficulties which tend to complicate the implementation of monolithic intersubband microcavities. The TM polarization selection rule, for instance, requires unusual geometries to achieve a high quality factor with effective light coupling, while the typical midinfrared wavelength results in rather large semiconductor layer thicknesses. Furthermore, linewidths and oscillator strengths seemed to be unsuitable for reaching a polaritonic regime. Yet the potential appeal is quite high, thanks to the possibility of externally controlling charge density and transition matrix elements and to the fast relaxation times. Moreover, intersubband transitions enjoy a close similarity to atomic ones, as a consequence of their ideally deltalike joint density of states and of the huge separation from continuum levels. Recent theoretical calculations have predicted that intersubband cavity polaritons can indeed be observed in planar resonators for oblique incidence by exploiting total internal reflection at the air interface [16]. Sufficiently large coupling with the radiation is in fact obtained using multiple QWs, with high carrier sheet densities in the 10^{11} cm^{-2} range.

In this paper we report the experimental observation of the vacuum-field Rabi splitting of an intersubband transition inside a planar microcavity with multiple 2DEGs embedded. The dispersion of the resulting intersubband polaritons has been measured through angle-resolved reflectance measurements using a prismlike geometry, and anticrossing energies of more than 10 meV have been observed up to room temperature. The experimental data have been found to be in good agreement with theoretical calculations performed in a transfer-matrix formalism.

The resonator implemented in this study is fully based on total internal reflection. In fact, distributed Bragg reflectors present at large incidence angles a much smaller reflectance value for TM polarization and would then have to be impractically thick. In our structure the radiation is instead confined between the semiconductor-air interface on one side (sample surface) and a low refractive index AlAs layer on the other. Above the critical angle this AlAs layer effectively acts as a low-pass filter for the light, as exemplified in Fig. 1(a): at 60° in a GaAs matrix a few micron thickness is enough to achieve reflectances of more than 90% for wavelengths shorter than 10 μm. The experimental geometry can then simply make use of the sample substrate, appropriately shaped in a wedge-prism configuration, to obtain the required incidence angle at the cavity surface, as shown in Fig. 1(b). The

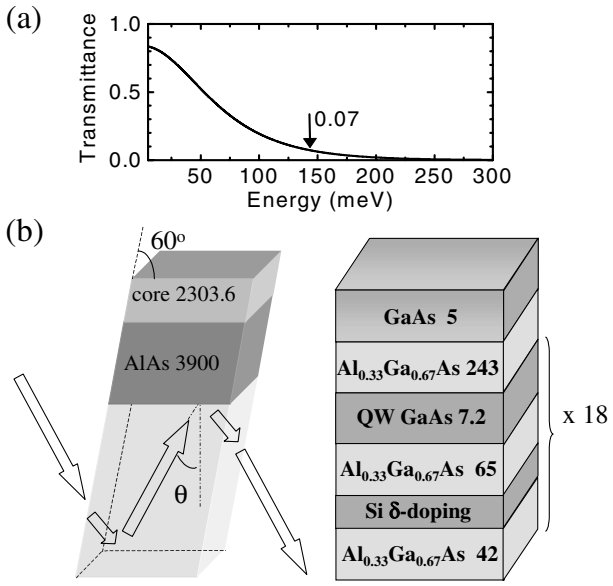

FIG. 1. (a) Calculated transmittance of a 3.9 μm-thick layer of AlAs embedded in GaAs at an angle of incidence of 60°; the arrow indicates the energy of the chosen intersubband transition (143 meV). (b) Schematic view of the prism-shaped microresonator. The large arrows represent the optical path of light in the substrate. The right-end part shows the structure of the active core; thicknesses are given in nm.

whole structure was grown by solid-source molecular-beam epitaxy on an undoped GaAs (001) substrate. It consists of a 3.9 μm-thick layer of AlAs followed by 18 nm wide GaAs quantum wells separated by 107 nm-thick $Al_{0.33}Ga_{0.67}As$ barriers; the latter are Si δ doped ($n_{Si} = 6 \times 10^{11}$ cm^{-2}) with 65 nm- and 42 nm-thick spacers below and above the wells, respectively. The well width was chosen in order to have the transition between the first and second subbands at about 9 μm wavelength, as short as possible but sufficiently far from the continuum and in a spectral region relatively free from atmospheric absorption. The last $Al_{0.33}Ga_{0.67}As$ barrier has a thickness of 243 nm to give the correct cavity length for 60° angle propagation. The latter was designed to be $\lambda/2$ of the transition; note however that the wave dephasing at both total internal reflections is different from π (particularly at the interface with the AlAs layer), which needs to be appropriately compensated in the cavity thickness. The sample was completed with a 5 nm GaAs cap layer to avoid Al oxidation. The growth conditions were optimized particularly in terms of the critical AlAs layer morphology, which could negatively affect light reflection at the interface and enhance the QW roughness. We checked the uniformity of the carrier density among the 18 QWs by measuring the Shubnikov–de Haas oscillations on van der Pauw structures at 1.5 K and magnetic fields up to 5 T. A single oscillation frequency was recorded, corresponding to a carrier sheet density of 4.17×10^{11} cm^{-2}. Before the realization of the final microcavity sample, preliminary transmission measurements were also performed on calibration structures to check the intersubband transition linewidth and to precisely monitor the cavity thickness. For the reflectance measurements the resonator was mechanically lapped into wedge-shaped prisms, with the facets at an angle of 60° with respect to the cavity plane (see Fig. 1). It was then soldered onto a copper holder and mounted onto the cold finger of a closed-cycle cryostat. The latter was inserted in the sample compartment of a Nicolet Fourier-transform infrared (FTIR) spectrometer, equipped with an Ever-Glo source and a liquid-nitrogen cooled HgCdTe detector. A metallic wire grid polarizer was inserted in the optical path to select either TM or TE polarization. By manually rotating the sample holder, the angle between the light beam and the prism facet could be varied, enabling us to change the incidence angle on the cavity surface θ around the central value of 60° defined by the prism shape.

Figure 2 shows the TM reflectance spectra in the frequency range of the intersubband transition measured at 10 K for different incidence angles. Two evident dips can be clearly identified, with a typical anticrossing behavior. By increasing the angle, the cavity mode is tuned across the intersubband one, until at resonance they mix and become strongly coupled, giving rise to intersubband polaritons with a splitting of around 14 meV. The resonance energy of the intersubband transition is about 142 meV, in very good agreement with the 143 meV computed with self-consistent calculations including dynamical many-body contributions such as the excitonic and depolarization shifts [11]. Its linewidth has been measured using a 45° wedged prism to exclude any possible cavity effect and a full width at half maximum (FWHM) of 5 meV has been recorded. This very low value attests the high quality and good uniformity of the quantum wells. On the other hand, the cavity mode has a FWHM of almost 15 meV. This value is larger than expected (a few meV) and is probably due to the nonideal reflectance of the cavity surfaces (roughness, etc.) and to the angle spread of the incident light beam. Inside the FTIR this is in fact focused on the sample with nearly $f/3$ optics and, although it was apertured to the lowest possible size, it is still not a parallel configuration. It is anyway worth pointing out that, at perfect anticrossing, the two fully mixed modes tend to share a nearly common linewidth, average of the two individual ones. For comparison, in the right inset of Fig. 2 we report a TE reflectance spectrum. Only the single cavity mode is visible, as in this polarization the intersubband transition is dipole forbidden, owing to the well-known selection rule [12]. As expected, the TE cavity mode is slightly broader than in the TM case and shifted to lower energies. In the left inset the energy position of the dips is plotted as a function of angle, to evidence the polariton anticrossing behavior. The dispersion appears to agree quite well with that of a simple Lorentzian dipole oscillator.

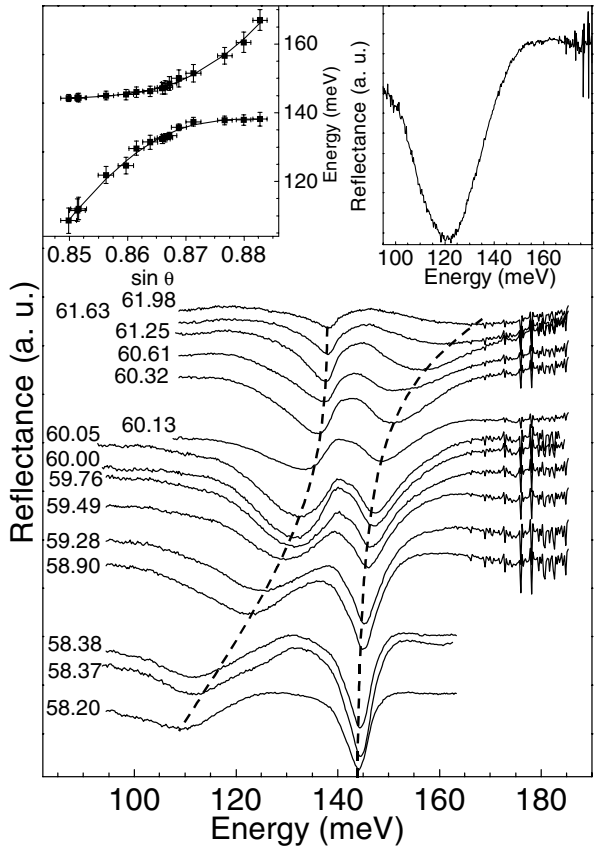

FIG. 2. Reflectance of the microcavity sample for different angles of incidence in TM polarization. The spectra were collected at 10 K, with a resolution of 2 cm^{-1}. The angle values refer to θ at the substrate-cavity interface; dashed lines are just a guide to the eye. The spectra are offset from each other for clarity. The rapid oscillations in the high energy portion are due to residual water vapor absorption in the purged FTIR system. In the left inset the experimental points corresponding to the energy position of the dips are reported. The solid lines are fitted with a standard dipole oscillator dispersion. The right inset contains a spectrum recorded under TE polarization; only the dip of the cavity mode appears.

In order to obtain a more quantitative description of the experimental data, we have performed a calculation of the structure reflectance using the transfer-matrix formalism [17]. In this approach every layer in the sample is characterized by a 2×2 matrix, which, through dielectric constant and thickness, fully accounts for the propagation of the electromagnetic wave across that layer. The optical response of the complete structure is then simply obtained by multiplying together the matrices corresponding to all the individual layers. The contribution of the intersubband transition within the 2DEGs has been considered by including in the dielectric permittivity ε of the quantum well layers an additional term in the form of a collection of classical polarized Lorentz oscillators:

$$\varepsilon(\omega) = \varepsilon_\infty + \frac{N_s e^2 f \sin^2\theta}{m_0 \varepsilon_0 L_{\text{eff}}} \frac{1}{(\omega_0^2 - \omega^2) - i\gamma\omega}, \quad (1)$$

in which ε_∞ is the quantum well high-frequency dielectric constant, N_s is the electronic sheet density, e the electronic charge, f the oscillator strength of the intersubband transition, $\hbar\omega_0$ its energy, m_0 the electronic mass, ε_0 the vacuum permittivity, and L_{eff} an effective QW thickness related to the confinement of the electronic wave functions [12]. The damping γ is a phenomenological factor nominally equivalent to the transition FWHM. The oscillator strength is related to the dipole matrix element d between the envelope functions of the two subbands: $f = (2m_0/\hbar)\omega_0 d^2$. In our case a value $d =$ 1.9 nm is computed using the proper orthonormalization procedure outlined in [18]. This form of the susceptibility obviously neglects the nonlocality of the 2DEG response; the latter would in general alter the line shape of the resonance and can introduce small corrections to its energy and strength. These are however minor effects, clearly not identifiable with the present experimental uncertainties.

In Fig. 3 we report the TM reflectance curves calculated in this way for various incidence angles. As one can see, this simple linear-dispersion model reproduces remarkably well the measured data and correctly describes the anticrossing behavior and polariton splitting. This should not be surprising in view of the known equivalence of the semiclassical and quantum description of coupled harmonic oscillators. Some discrepancy arises from the

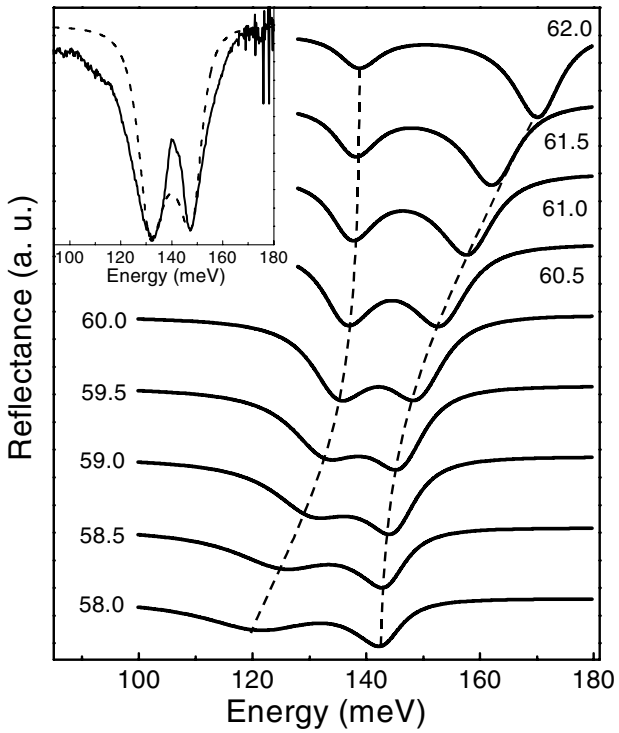

FIG. 3. TM reflectance of the sample as obtained at different incidence angles using the simulation procedure described in the text. The spectra are offset from each other for clarity. In the inset we report a comparison between the experimental and calculated spectrum at the resonance angle of 60.05°.

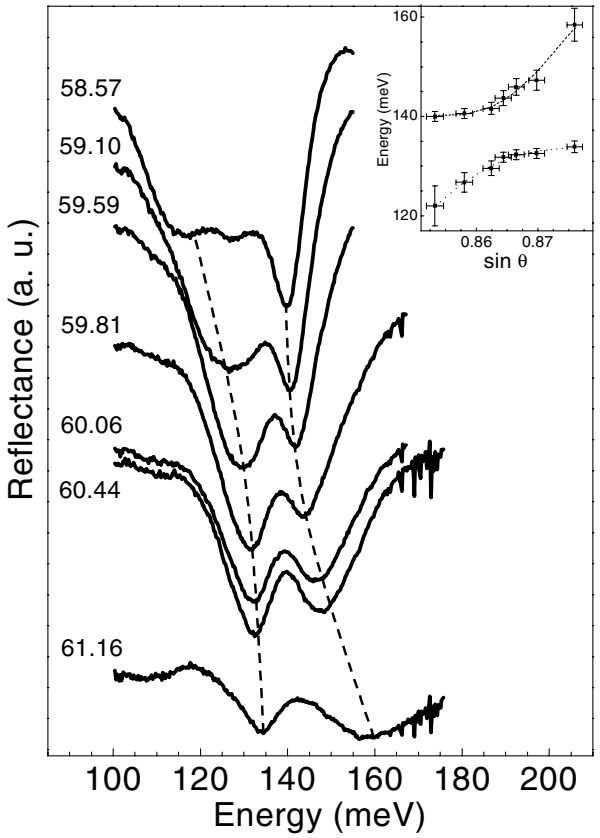

FIG. 4. The structure TM reflectance as recorded at 300 K for different angles of incidence. The spectra show a polariton splitting of about 11 meV, smaller than at low temperature. The third dip appearing in the 58.57° curve is probably an artefact due to background subtraction. In the inset we plot the energy position of the dips as a function of angle; the dotted line is a fit with a Lorentzian oscillator dispersion.

angle spread of the incident radiation which is not included in the calculation. To partly compensate for it, the cavity mode has been artificially broadened by reducing the reflection at the AlAs interface. The value of the vacuum-field Rabi splitting can be tuned to the observed one by fitting the confinement length L_{eff}. This yields $L_{\text{eff}} = 7.8$ nm, as expected a thickness slightly larger than the well width.

The polaritonic dispersion of the intersubband cavity modes remains clearly visible up to room temperature. In Fig. 4 we report the reflectance of the structure as measured at 300 K for different incidence angles. As in the case of cryogenic temperatures, the anticrossing is evident, with a well-defined polariton splitting of approximately 11 meV. This value is slightly lower than at 10 K, probably a consequence of charge redistribution between the subbands. Note also that, since the intersubband transition is a bit shifted to lower energies [19], the perfect resonance with the cavity mode occurs at a different angle with respect to low temperatures.

In conclusion, we have observed the vacuum-field Rabi splitting of the intersubband transition in two-dimensional electron gases within a planar microcavity. The dispersion of the resulting intersubband polaritons has been measured up to 300 K and modeled in a semiclassical scheme. These excitations should be of great interest both for fundamental studies of parametric light amplification and condensation phenomena in electronic systems and for the realization of novel ultrafast devices as well.

We would like to acknowledge Stefano Luin, Giuseppe La Rocca, and Fabio Beltram for precious help and useful discussions. The work was supported in part through the PAIS project ICONS of the INFM.

*Electronic address: tredicuc@nest.sns.it

[1] S. Haroche and D. Kleppner, Phys. Today **42**, No. 1, 24 (1989).
[2] J. M. Raimond, M. Brune, and S. Haroche, Rev. Mod. Phys. **73**, 565 (2001).
[3] C. Weisbuch, M. Nishioka, A. Ishikawa, and Y. Arakawa, Phys. Rev. Lett. **69**, 3314 (1992).
[4] G. Khitrova, H. M. Gibbs, F. Jahnke, M. Kira, and S. W. Koch, Rev. Mod. Phys. **71**, 1591 (1999).
[5] R. Rapaport, R. Harel, E. Cohen, A. Ron, E. Linder, and L. N. Pfeiffer, Phys. Rev. Lett. **84**, 1607 (2000).
[6] M. Saba, F. Quochi, C. Ciuti, U. Oesterle, J. L. Staehli, B. Deveaud, G. Bongiovanni, and A. Mura, Phys. Rev. Lett. **85**, 385 (2000).
[7] A. Tredicucci, Y. Chen, V. Pellegrini, M. Börger, L. Sorba, F. Beltram, and F. Bassani, Phys. Rev. Lett. **75**, 3906 (1995).
[8] P. Kelkar, V. Kozlov, H. Jeon, A. V. Nurmikko, C. C. Chu, D. C. Grillo, J. Han, C. G. Hua, and R. L. Gunshor, Phys. Rev. B **52**, R5491 (1995).
[9] M. Saba *et al.*, Nature (London) **414**, 731 (2001).
[10] H. Deng, G. Weihs, C. Santori, J. Bloch, and Y. Yamamoto, Science **298**, 199 (2002).
[11] S. Luin, V. Pellegrini, F. Beltram, X. Marcadet, and C. Sirtori, Phys. Rev. B **64**, 041306 (2001).
[12] *Intersubband Transitions in Quantum Wells: Physics and Device Applications I*, edited by H. C. Liu and F. Capasso, Semiconductors and Semimetals Vol. 62 (Academic Press, San Diego, 2000), p. 126.
[13] M. Beck, D. Hofstetter, T. Aellen, J. Faist, U. Oesterle, M. Ilegems, E. Gini, and H. Melchior, Science **295**, 301 (2002).
[14] R. Köhler, A. Tredicucci, F. Beltram, H. E. Beere, E. H. Linfield, A. G. Davies, D. A. Ritchie, R. C. Iotti, and F. Rossi, Nature (London) **417**, 156 (2002).
[15] C. Gmachl, J. Faist, F. Capasso, C. Sirtori, D. L. Sivco, and A. Y. Cho, IEEE J. Quantum Electron. **33**, 1567 (1997).
[16] A. Liu, Phys. Rev. B **55**, 7101 (1997).
[17] M. Born and E. Wolf, *Principles of Optics* (Pergamon Press, New York, 1980).
[18] C. Sirtori, F. Capasso, J. Faist, and S. Scandolo, Phys. Rev. B **50**, 8663 (1994).
[19] B. C. Covington, C. C. Lee, B. H. Hu, H. F. Taylor, and D. C. Streit, Appl. Phys. Lett. **54**, 2145 (1989).